

Experimental investigation of horizontal axis wind turbine dynamic stall in a wind tunnel

Pascal Hemon, Domenico Olivari and Martin Wurmser

Von Karman Institute for Fluid Dynamics, 72, Chaussee de Waterloo, 1640 Rhode-st-Genese, Belgium

Summary

This paper presents the results of the study of the dynamic stall on horizontal axis wind turbines. Pressure values are measured at fixed points on the suction side of the blade using Kulite transducers, and the effective blade angle using a crossed hot-wire anemometer installed upstream of the leading edge. Results put into evidence the importance of unsteady phenomena.

1. Introduction

Blade stall is increasingly becoming the standard mode of power regulation of medium and large wind turbines. Therefore stall behaviour must be better understood in real working conditions that are unsteady most of the time.

In addition, wind direction variations change the yaw angle and this may lead also to a dynamic stall on the blades at frequency equal to the rotational velocity of the rotor.

To investigate this problem, the CEE has launched under the Joule program a collaborative research to which the VKI participates. The study which is presented here reports the activity of VKI which has been charged to study the problem on reduced scale models in its large atmospheric wind tunnel L1B.

The first objective is to study the scale effect by making a comparison of values obtained on a scale model and on the real wind mill. The second objective of the research is to validate computer codes that could also take into account the case of fully or partially stalled blades, during yawed operation.

The models, which can be mounted with a variable yaw angle in the test section, will then undergo dynamic stall, that can be first described by measuring the pressure at the surface of a blade and the relative angle between the blade and the flow near the leading edge.

2. Wind turbine facility

2.1. The models

Two models have been designed and are being tested in the atmospheric wind tunnel L1B, which has a rectangular test section of 3×2.50 m. According to the dimension of the tunnel, the rotor diameter has been chosen to be less than 1.4 m [1].

The first windmill has two nontwisted and nontapered blades. It has a 1.2 m diameter equipped with a NACA 63₂215 profile. The chord is 100 mm and it is scaled 1/16 referring to the Risø one [2]. The second windmill has two blades tapered but nontwisted. It is 1.4 m diameter equipped with a NACA 4415 profile. It is scaled 1/2 referring to the Crandfield one [3]. They are design to achieve about 500 rotations per minute, with a wind of 7–9 m/s.

2.2. The rotor, the pitch control system (PCS)

The blade support mechanism comes from an helicopter model but it has been modified to accept larger instrumented blades. The mechanical energy produced by the wind mill is dissipated in an alternator through a vertical axis.

The axis of the rotor is hollowed to host the electrical wires connecting the instruments on the blade to the external equipment through slip-rings. A bevel gear is mounted on this axis to transmit the power to a vertical axis. The pitch setting angle is variable and can be changed with a small motor, remotely controlled, mounted at the top of the rotor head. The rotating velocity of this motor was chosen to obtain a very accurate control of the pitch (less than 3 min). Two micro-switches are mounted at predetermined positions on the moving part, to act as displacement limiting safety devices. A displacement sensor whose response is read on a digital voltmeter acts as pitch angle measurement.

2.3. The load control system (LCS)

An alternator, fixed under the wind tunnel, is actioned by the windmill. By varying the excitation current, and so the load on the blade, it is possible to regulate the rotationnal velocity of the model.

The ratio of the gears between the alternator and the windmill is 41.17 which is an irrational value. It allows then to avoid mechanical vibration of the alternator at a frequency proportional to twice the rotor speed, and so, avoid interferences on the measured aerodynamic effect. With this system, it is possible to measure the power output of the windmill, by measuring the alternator power output.

An emergency braking system is mounted: The alternator is in auto-excited mode, loaded by a small resistance.

2.4. Aerodynamic considerations

For obvious reasons, and since this is the object of the research, the Reynolds number of the models is one order of magnitude lower than the real one, however the tip speed ratio (ratio of the rotational velocity over the wind velocity) is respected.

The rotor can be yawed up to $\pm 40^\circ$ in order to simulate of axis operation and create the unsteady effects on the blade at rotor speed frequency. For any yaw angle, it is possible to calculate a geometrical angle of attack α , variable along the span. Calling γ the yaw angle, ϕ the azimuth (position of the blade in the rotation), λ_r the local speed ratio and if β is the pitch setting angle, the local geometrical angle of attack is given by:

$$\alpha = \arctan \left(\frac{\cos(\gamma)}{\lambda_r + \sin(\gamma) \cos(\phi)} \right) + \beta.$$

For positive yaw angles, α is maximum for $\phi = 180^\circ$ and minimum for $\phi = 0^\circ$ (positive yaw angle), and oscillates between these values. It is interesting to notice that the amplitude of oscillation decreases when λ increases.

Theory shows that it is possible, at large yaw angles to have oscillations of angle of attack which will provide the dynamic stall even with small negative pitch setting angle.

3. Blade manufacturing

Several constraints have to be respected to built the blades. First, a compromise has to be found between the weight and the rigidity. Second, the building procedure must take into account the fact that there are instruments mounted inside the blade. Because there were two different types of blades (not tapered and tapered), two different techniques have been used.

3.1. NACA 63₂215 windmill

The middle of the blade consists of foam (ROHACELL 110) which has a density of 0.11; the leading and trailing edge are made with balsa soaked in polyester, in order to increase the surface hardness; the surface is made of plywood (0.4 mm thick), glued inside a vacuum bag to have a uniform pressure distribution. Instruments are mounted inside the foam before the last piece of plywood is stuck. The final operation is to sand the profile to obtain the real shape with the smallest possible roughness. The shape of the foam and the final one are controlled with especially designed metal gauges.

With such a device to built the blade, the maximum accuracy that could be expected is of the order of 0.5 mm.

3.2. NACA 4415 windmill

As the profile of each blade is tapered, it is not possible to use the same technique than for the previous one. That is the reason why two moulds have been built, the first one for the suction side of the blade, the second one for the pressure side. Each side of the blade is then made separately out of resin and carbon fiber and consists in a thin skin. The instrumentation takes place inside the suction side and the two parts are finally put together.

It is then possible to define four blades as follows:

blade number 1

Naca 63₂ 215 pressure transducers at 75% of the radius hot wire at 77% already built, tested

blade number 2

Naca 63₂215 pressure transducers at 35% hot wire at 32% already built

blade number 3

Naca 4415 pressure transducers at 75% hot wire at 35% not built

blade number 4

Naca 4415 pressure transducers at 35% hot wire at 75% already built

4. Instrumentation

4.1. Pressure transducers

4.1.1. Choice

To instrument the wing it was decided to use Kulite-type semi-conductor strain-gauge transducers for the following reasons:

- a high frequency response;
- small dimensions (2.2 mm in diameter and 6 mm long);
- a zero shift/temperature compensation module (also very small);
- small pressure sensitive area;
- low sensitivity to gravity;
- good experience with them at the VKI.

4.1.2. Connections

Because of the small thickness of the blade, the pressure probes cannot be flush mounted. The sensitive surface is on the top of the 6 mm cylinder. So, connections were designed in order to obtain a cut-off frequency of the system pipe + transducer higher than 1000. To realize the objective, the diameter of the pipe has been kept constant from the tap at the surface to the transducer, in order to avoid any cavity effect, and special care has been taken to that point during the manufacturing. The section of the pipe is also equal to the pressure sensitive area of the transducer, and is 1.2 mm in diameter. The frequency response of the system has been tested to verify that the objectives were achieved.

On each blade, transducers are mounted at the same radius in order to have

a centrifugal effect of the same value. The differential pressure pipes are connected all together to go down to the root of the blade. A common pipe is connected to a total pressure tap fixed on the rotation axis. The flow there is supposed not much perturbed and the pressure measured close to a constant value, the wind total pressure.

In reality the alignment of the tube with the rotation axis is not perfect, and also in yawed operation the main flow has an incidence with the tube. Taking apart these defaults, and knowing that the mean value of the pressure is not the most important data to measure, this solution for the differential pressure reference seems good. Locations of taps are 15%, 25%, 38%, 52% and 74% of the chord, for the blade number one. For the other blades, pressure taps are at 15%, 25%, 35%, 55% and 75% of the chord.

4.2. Angular position of the blade

The angular position means the angle made by the blade with a vertical axis, origin is taken when the instrumented blade is vertically down. To record it, an optical disk is mounted on the rotating axis near the alternator. It has 120 holes counted by an optical sensor and output signal increases one step at each hole detected. The trigger for data acquisition is an optical sensor and has also the role of setting the output signal to zero at each rotation.

4.3. Crossed hot wire

In order to measure the local flow angle near the blade leading edge, a crossed hot wire anemometer has been installed on the leading edge of each wind mill blade. Those two wires allow to measure the velocity magnitude and direction close to the blade. This measured angle can be then compared to the calculated one.

5. Data acquisition system

5.1. Connection to DAS 20

To record the data, a DAS20 Data Acquisition System is installed in a PC computer. Six channels are used: one for the angular position of the instrumented blade, the five others for the pressure transducers and hot wire. To obtain the signal from the rotating blade, slip-rings are used which can connect up to twelve wires. Each blade has five pressure transducers each with four connection-wires, and one crossed hot wire with four wires, so twenty four lines, have to be used. To overcome this it was decided to do twice the same test, one with five pressure taps connected and the other with the crossed hot wire and three pressure tap connected. Even with this procedure, all the pressure transducers power inputs have had to be put in common.

Another drawback of these transducers is their low sensitivity. However, this can be corrected since amplifiers for the pressure transducers have a gain

and offset adjustment and the input voltage of the acquisition card can be modified by software. So after optimisation, one arrive at a gain of the order of 2000 Pa/V.

5.2. External/internal trigger

Acquisition is made in "block scan mode" which means that the six channels are recorded one after the other at a rate of 100 kHz. However, the time interval between each block record is the sampling frequency, and can be controlled by internal or external trigger.

Internal trigger is done by the internal timer of the PC, and then this sampling frequency is constant, accurate and adjusted with software at the beginning.

External trigger can also be used for synchronization of the pressure records with the position of the blade when required. The signal for triggering is the counter output signal delivered by the optical disk system.

6. Data processing

6.1. First settings

Measurements with internal trigger were performed in order to detect vibrations in the windmill, by computing the power spectrum of the pressure signals. These tests were useful during the beginning of the measurements program, specially for detecting the 50 Hz component. Only few configurations were tested, with the rotational speed as the main and obvious parameter.

Different programs were developed for signal processing. They are written in C language and run on a PC. It is recommended to use at least a 80286 because of the execution time.

6.2. Power spectrum and filters

To compute the power spectrum, an other program was developed and named SPECTRE. It works only for tests that have been made with the internal trigger, because only in that case the sampling frequency is constant. The computation uses the FFT algorithm found in ref. [4]. However, a filter could have been necessary because of the 50 Hz component in the signal, therefore a digital filter have been introduced in the data processing step. This is an additional program named FILTRE, and must be called after SPECTRE. It is a band cut filter. Analog low pass filters are included in the amplifiers elements.

6.3. Mean curves

All the results are computed as the mean value. The plot of the pressure and angle of attack are then reduced to easily readable curves. This is different with the instantaneous values, where a scatter cannot be avoided. Typical val-

ues are 16 rotations averaged and with a resolution of 2040 points per channels per rotation.

7. Results

The measurements presented in this chapter have been obtained with blade number one which is instrumented at 75% of the radius on the NACA 63₂-215 profile.

7.1. Tests list

The tests have been done for six different values of tip speed ratio (between 3.55 and 4.5), with two different values of wind velocity (8.0 and 8.5 m/s). Yaw angles were -40° , $+20^\circ$ and $+40^\circ$ and few measurements were made with a larger support tower in order to observe its influence.

7.2. Format of results

Each presented test has four plots, the first one giving the test conditions, the second one the pressure versus geometrical angle of attack (five curves), the third and the fourth respectively pressure and real angle of attack versus azimuth angle.

In a frequency analysis test, results are presented on one sheet only, where six power spectrum are plotted, first one for the angle α_{geo} , and the five others for the pressure.

The pressure is plotted in pascal, between the values -150 to 150 . In fact, because uncertainty on the mean level is very high, from the pressure measured is subtracted the average pressure which is the result of the addition of all values, and divided by the number of data. Therefore, in all plots, pressure is located around zero values, which is also a very convenient way for comparing dynamic tests one with an other. In term of geometrical angle of attack, the range is from 0° to 15° . For the frequency plots, the frequency span is 100 Hz.

7.3. Typical results

7.3.1. Pressure

Typical results are shown in Fig. 1 for a wind velocity of 8 m/s, a tip speed ratio of 3.56 and a yaw angle of 20° .

7.3.2. Angle of attack

In Fig. 2 are presented two angles of yaw (20° and 40°).

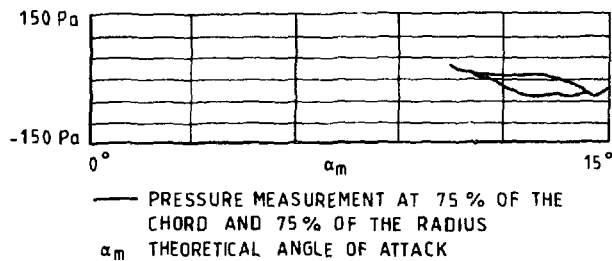


Fig. 1.

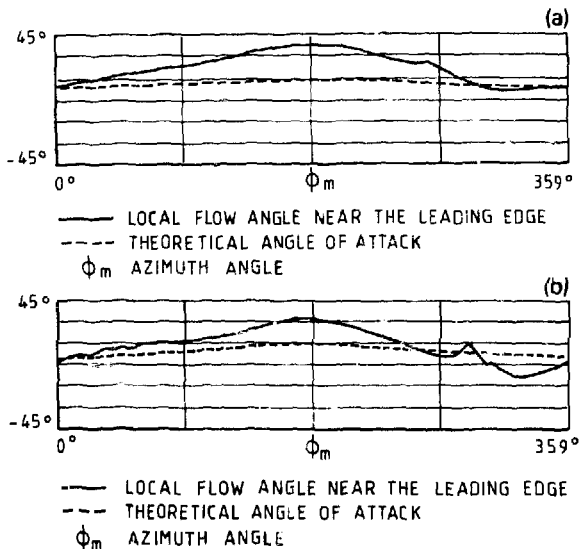


Fig. 2.

7.4. Analysis

7.4.1. Introduction

In all tested conditions, the pressure fluctuations are of the order of 300 Pa which can be compared with the local velocity (about 24 m/s) that is 350 Pa in term of dynamic pressure. Then the order of magnitude of pressure fluctuations due to yawed operation (in stalled conditions) is the same as the dynamic pressure.

One can observe also that these fluctuations decrease along the chord, like a static typical pressure curve.

7.4.2. Tip speed ratio effect

One has seen previously that the yaw angle has also an effect on the pressure signals, because it creates itself the unsteady flow on the blade. However, during yawed condition, the tip speed ratio plays the most important role in stall behaviour because its value takes a part in the angle of attack fluctuations. Whether it is small, amplitude of oscillations of α are large, and they decrease when λ increases.

7.4.3. Reynolds number effect

Tests were done with same tip speed ratio but with different velocities ($v=8$ and 8.5 m/s). As expected, pressure response curve have the same shape for all taps.

The general conclusion of these comparisons is that a dynamic pressure increase induce an increase of the amplitude of fluctuations, without changing the shape of curves which is done only by yaw angle or tip speed ratio variation.

7.4.4. Reduced frequency

The reduced frequency can be calculated for the present case of 3D study. It is given by

$$k = \frac{\pi f_{\text{typ}} C}{W},$$

which with the windmill parameters can be expressed as

$$k = \frac{C\lambda}{2R(1+\lambda^2)^{1/2}}$$

One can see then that for λ large enough, the reduced frequency is given by the maximum value:

$$k_m = \frac{C}{2R} = 0.111 \quad (\text{at } 75\%).$$

For all tests, λ is larger than 1 and then the order of magnitude of the reduced frequency is 0.083 for tip of blades.

7.5. Small/large support tower

A few tests have been made with a large tube fixed on the support tower of the windmill. The goal of these tests is to detect the influence of this tower on the pressure signals.

The small tower, that is the normal one, has 42 mm of diameter. The distance between the tower axis to the rotation plan is 165 mm, which gives 4 times the diameter. The tube for the large tower is 100 mm of diameter, then distance from its axis to the rotation plan is 1.65 times the diameter.

It is easier to compare the curves pressure versus azimuth because the tower is located at $\phi=0$. The first observation is that effect of the tower is really smaller with a negative yaw angle than with a positive one. This can be explained because the upstream flow in case of negative yaw is coming from an area which is shifted relatively to the support tower position. This shift is due to the rotating blades, and by this way, it is obvious that the inflow in case of positive yaw is also shifted, but then is coming from the area that is located

just in front of the tower. The tower effect is also larger with a higher tip speed ratio, which is due also to the increase of the rotating component.

Furthermore, effect of tower is more significant near the leading edge and decreases along the chord. On the pressure tap number 5, at 74% of the chord, the difference between pressure signals with large or small tower does not exist or is very small.

For positive yaw, the change in pressure response is located around the zero azimuth position, and particularly there is a peak of pressure at $\phi = 30$, which is higher with the large tower, while a valley is amplified at $\phi = 330$. Therefore, even in the tests with the small tower, it is possible to interpret this peak and this valley as an effect due to the tower.

In plots of pressure versus angle of attack, then these differences appear in the small values of α_{geo} , because in case of positive angle, this area corresponds to the area $\phi = 0$. Therefore, the small loop for pressure tap 2 is amplified with the large tower, which allows to say that this loop is due to the support tower effect.

7.6. Conclusion

Pressure and real angle of attack measurements have been made at 75% of the radius of the first wind mill. Different tip speed ratio and different Reynolds number have been explored and the effect of the support tower has also been shown.

As the other wind mill is now built, it will be possible to finish the construction of a library of values to be compared with results obtained on real facilities.

References

- 1 C. Depasse, Régulation et automatisation de l'angle de calage des pâles d'une éolienne en fonction de la vitesse du vent, superviseur: D. Olivari, U-VKI 1982-12 (ULB)
- 2 H. Aagaard Madsen, Raw Data Overview, Novembre 1990.
- 3 Cranfield Institute of Technology, An experimental investigation of HAWT aerodynamics in natural conditions, July 1990.
- 4 E. Oran Brigham, The Fast Fourier Transform (Prentice-Hall, Englewood Cliffs, NJ).